

Supporting Information of

Hybrid polymers bearing oligo-L-lysine(carboxybenzyl)s: investigations of secondary structure formation in 2,2,2- trifluoroethanol

Merve Basak Canalp^a and Wolfgang H. Binder*^a

Table of contents

- I. ¹H-NMR analyses of oligo-L-lysine(Z)s and ADMET polymers
- II. MALDI-ToF MS analyses of oligo-L-lysine(Z)s and ADMET polymers
- III. CD spectroscopy investigations in TFE
- IV. IR spectroscopy investigations in TFE
- V. Preparative GPC analyses of ADMET polymer A-[Lys_{n=3}]_{m=3}
- VI. Preparative GPC analyses of ADMET polymer A-[Lys_{n=24}]_{m=4}

I. ^1H -NMR analyses of oligo-L-lysine(Z)s and ADMET polymers

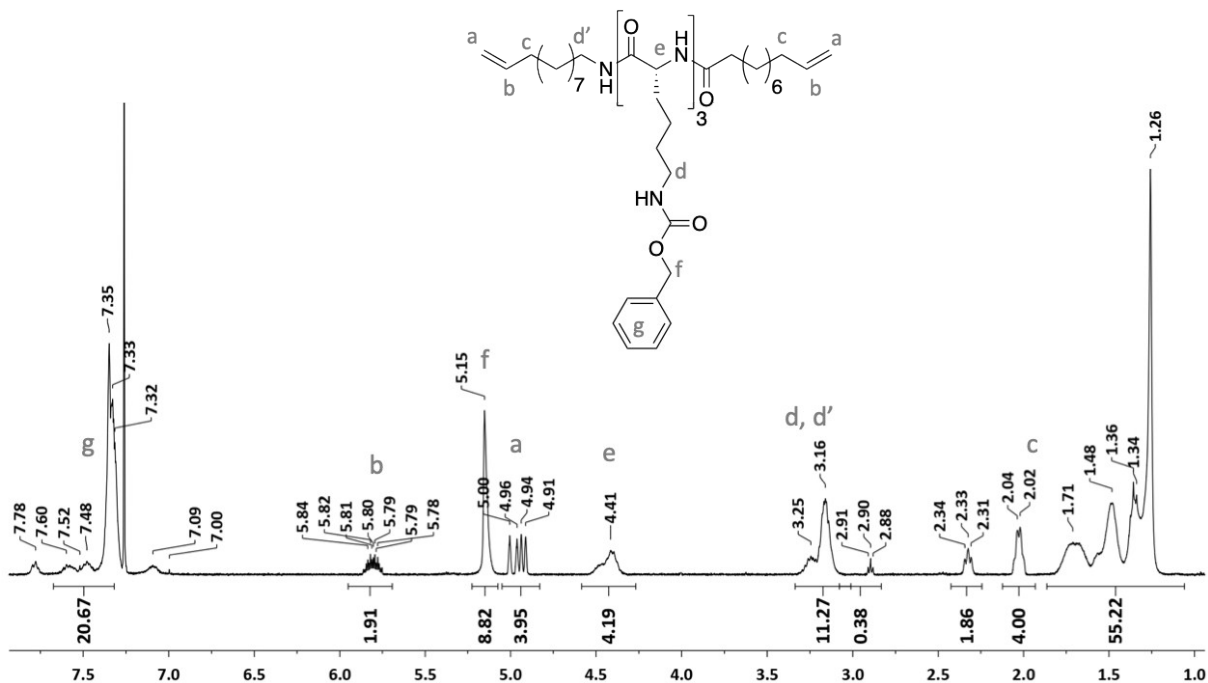


Figure 1S. ^1H -NMR of $\text{Lys}_{n=3}$ (in CDCl_3 and 15 vol.% TFA).

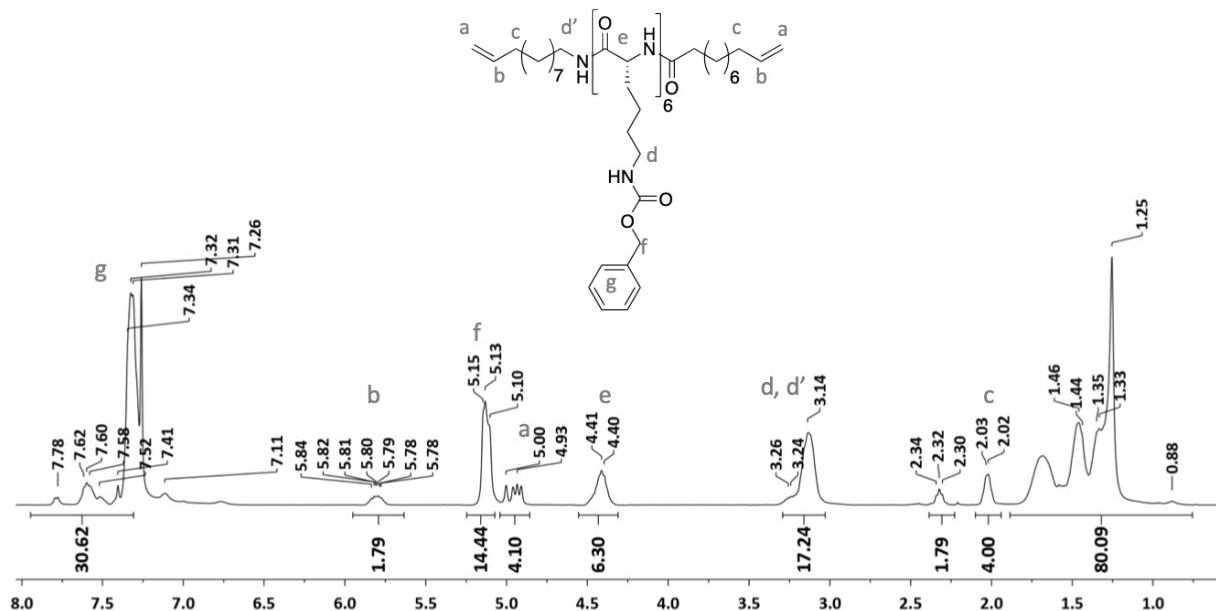


Figure 2S. ^1H -NMR of $\text{Lys}_{n=6}$ (in CDCl_3 and 15 vol.% TFA).

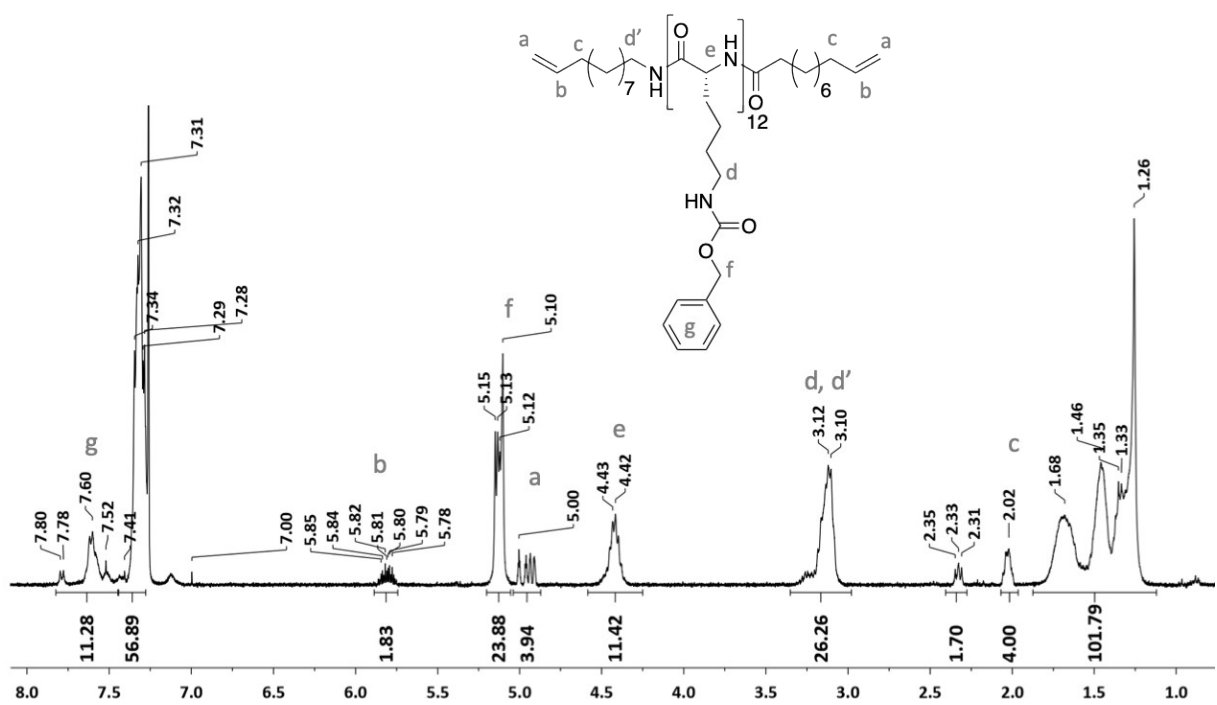


Figure 3S. ^1H -NMR of Lys_{n=12} (in CDCl₃ and 15 vol.% TFA).

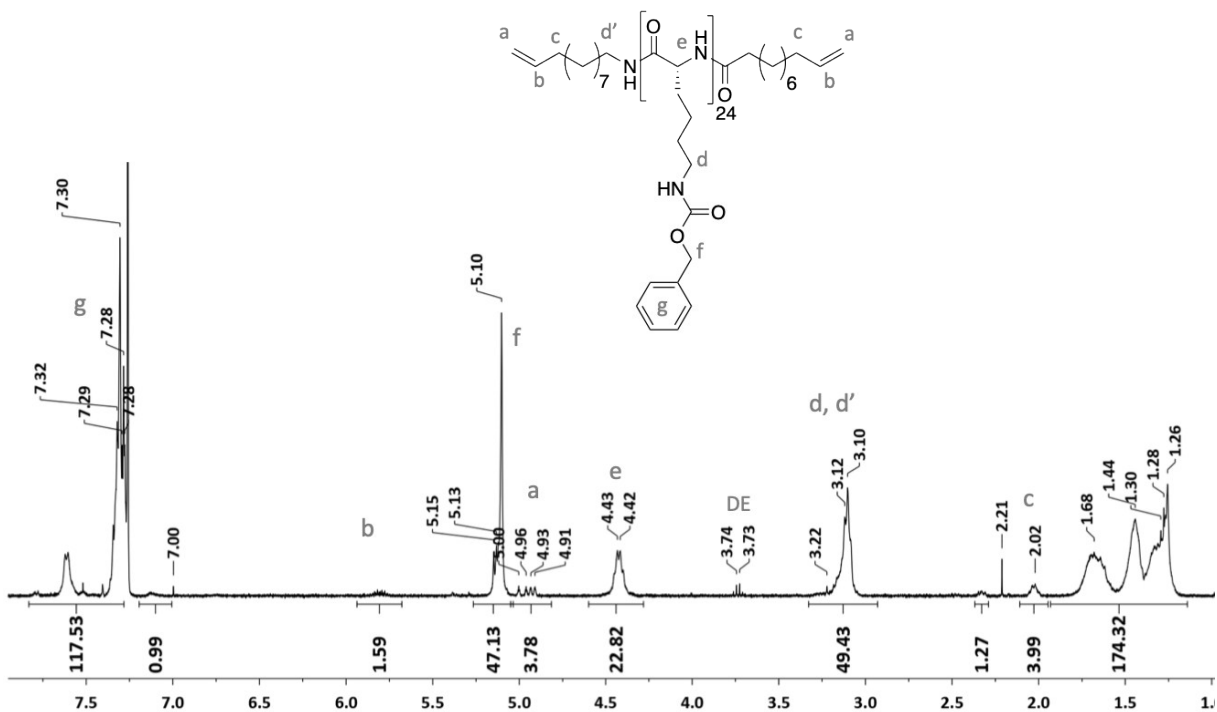


Figure 4S. ^1H -NMR of Lys_{n=24} (in CDCl_3 and 15 vol.% TFA).

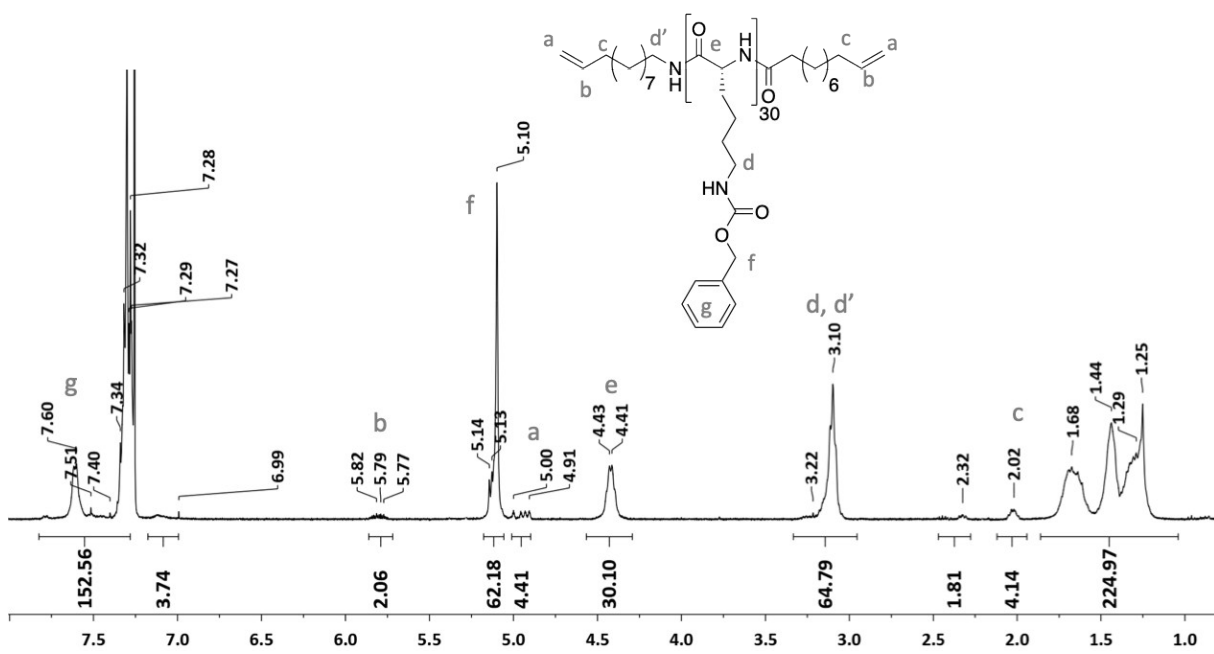


Figure 5S. ^1H -NMR of Lys_{n=30} (in CDCl₃ and 15 vol.% TFA).

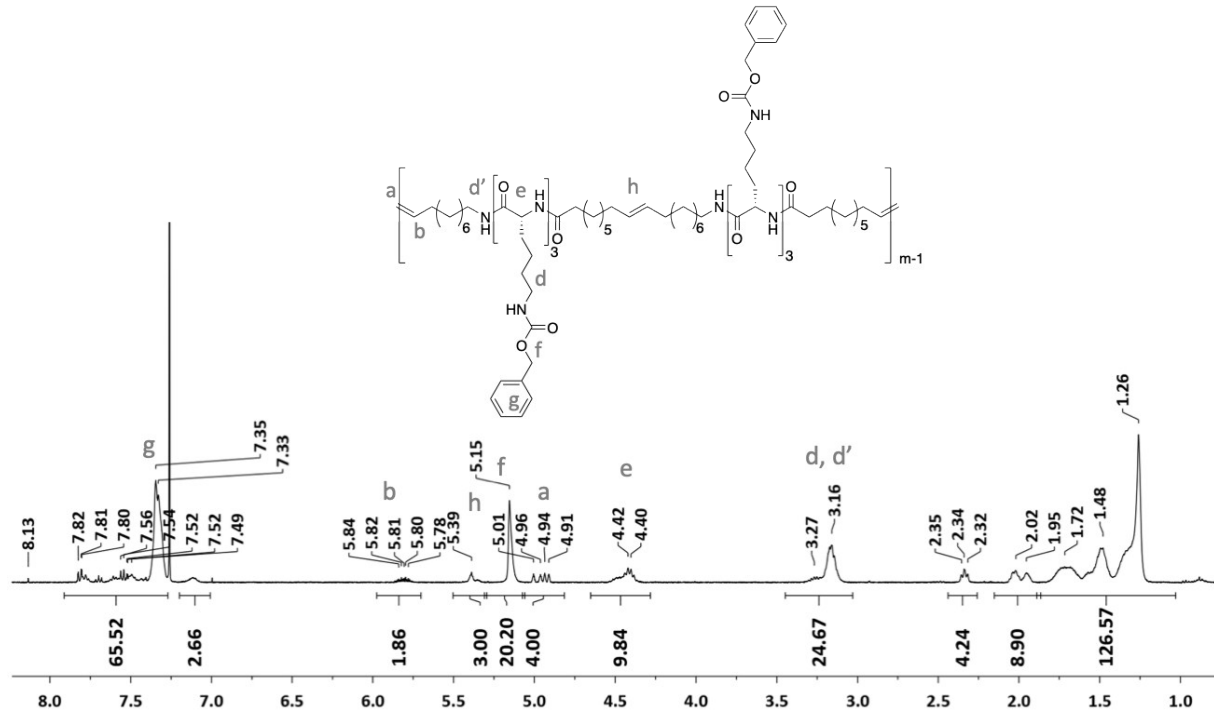


Figure 6S. ^1H -NMR of A-[Lys_{n=3}]_{m=3} (in CDCl₃ and 15 vol.% TFA).

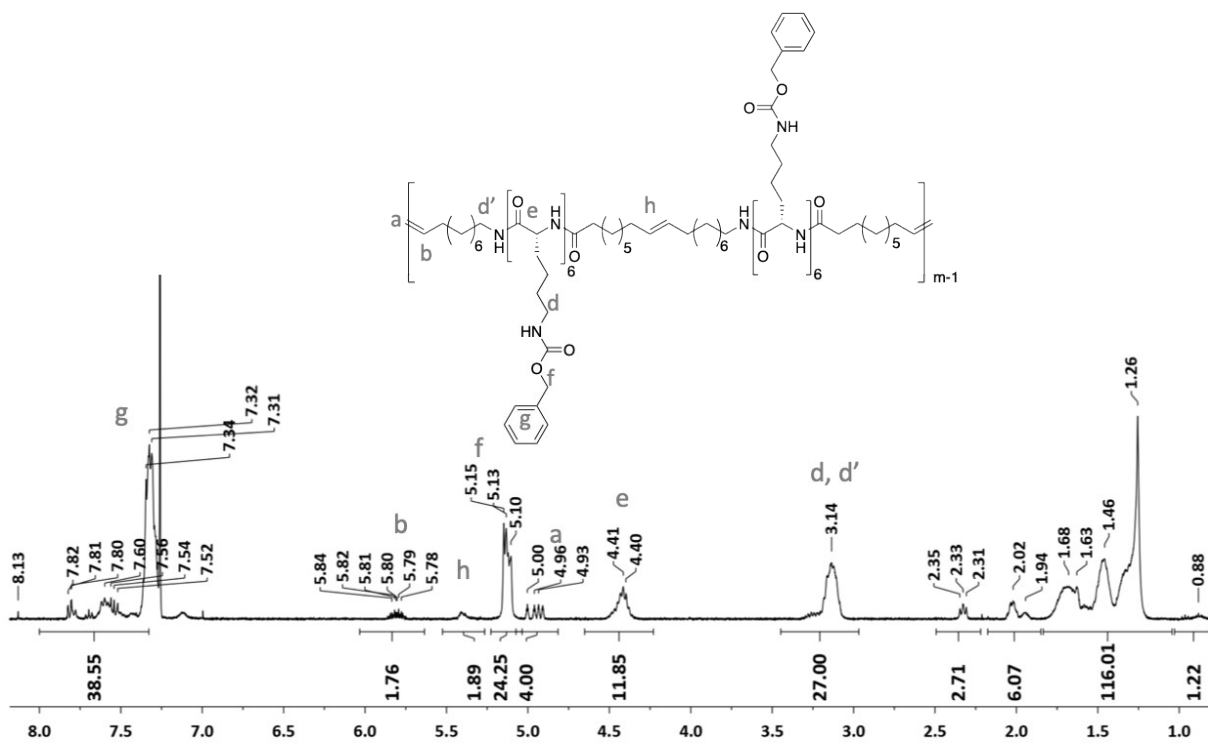


Figure 7S. ^1H -NMR of A-[Lys_{n=6}]_{m=2} (in CDCl₃ and 15 vol.% TFA).

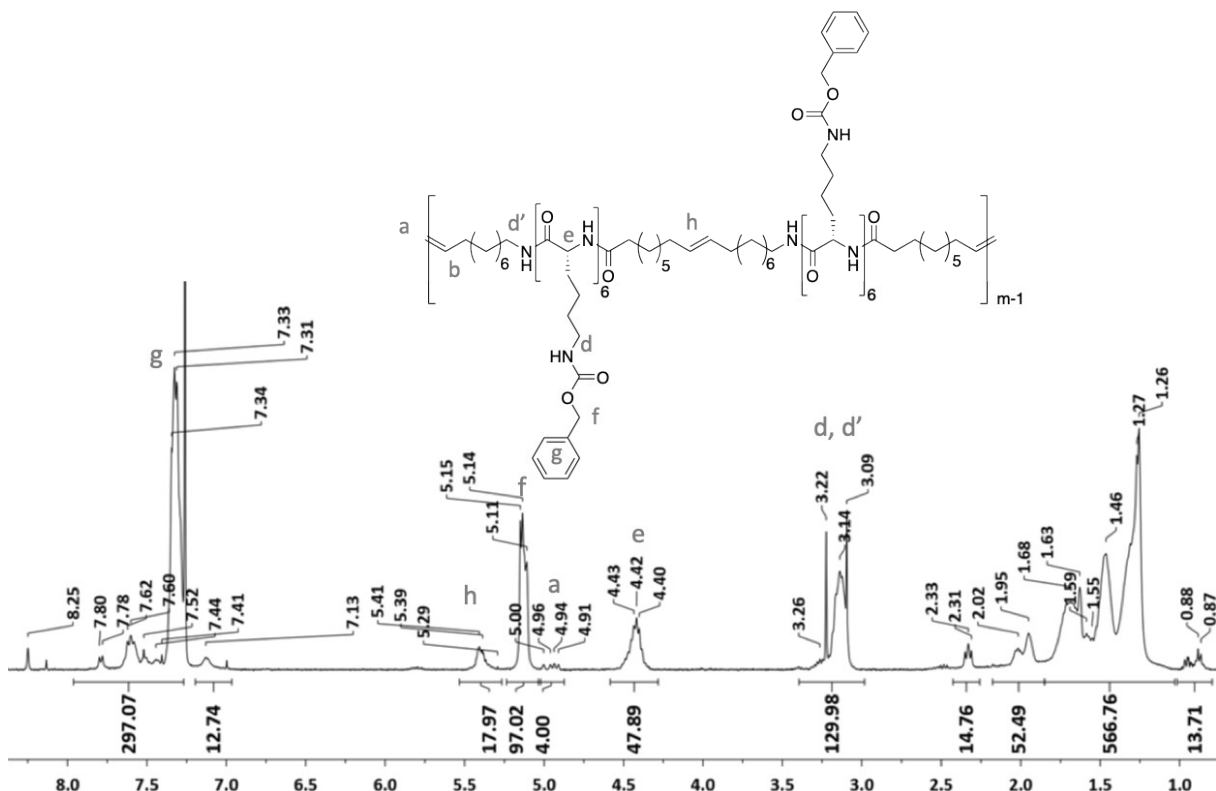


Figure 8S. ^1H -NMR of A-[Lys_{n=6}]_{m=12} (in CDCl₃ and 15 vol.% TFA).

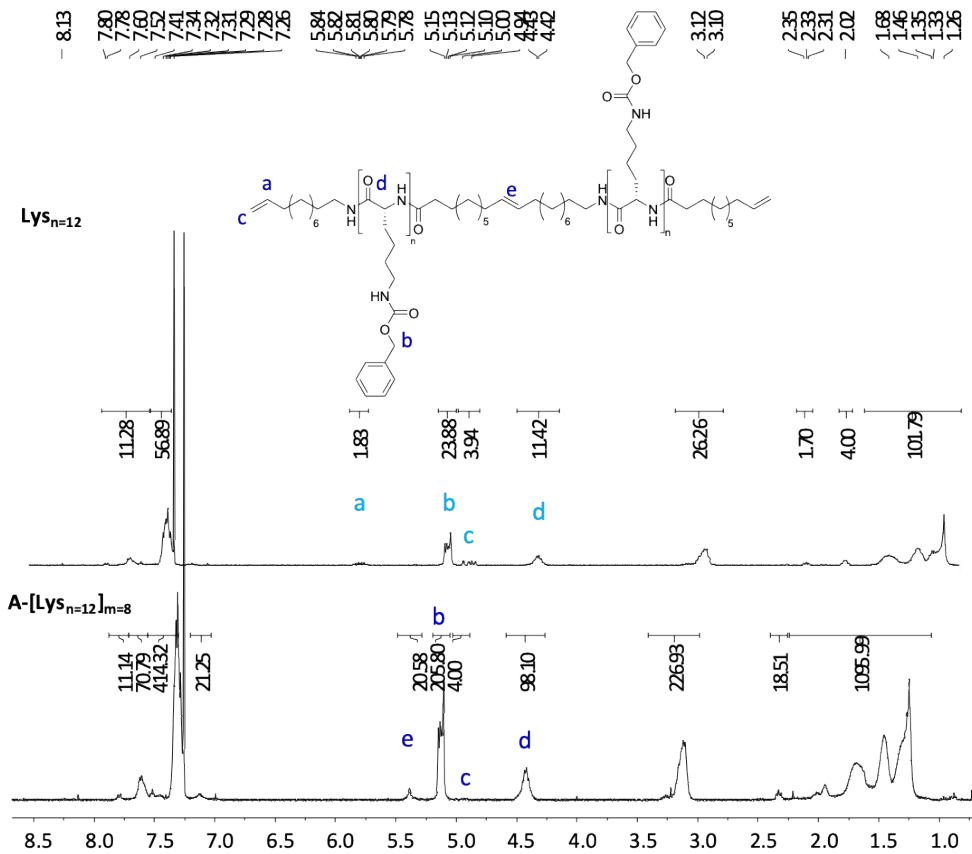


Figure 9S. ^1H -NMR of Lys_{n=12} and A-[Lys_{n=12}]_{m=8} (in CDCl₃ and 15 vol.% TFA).

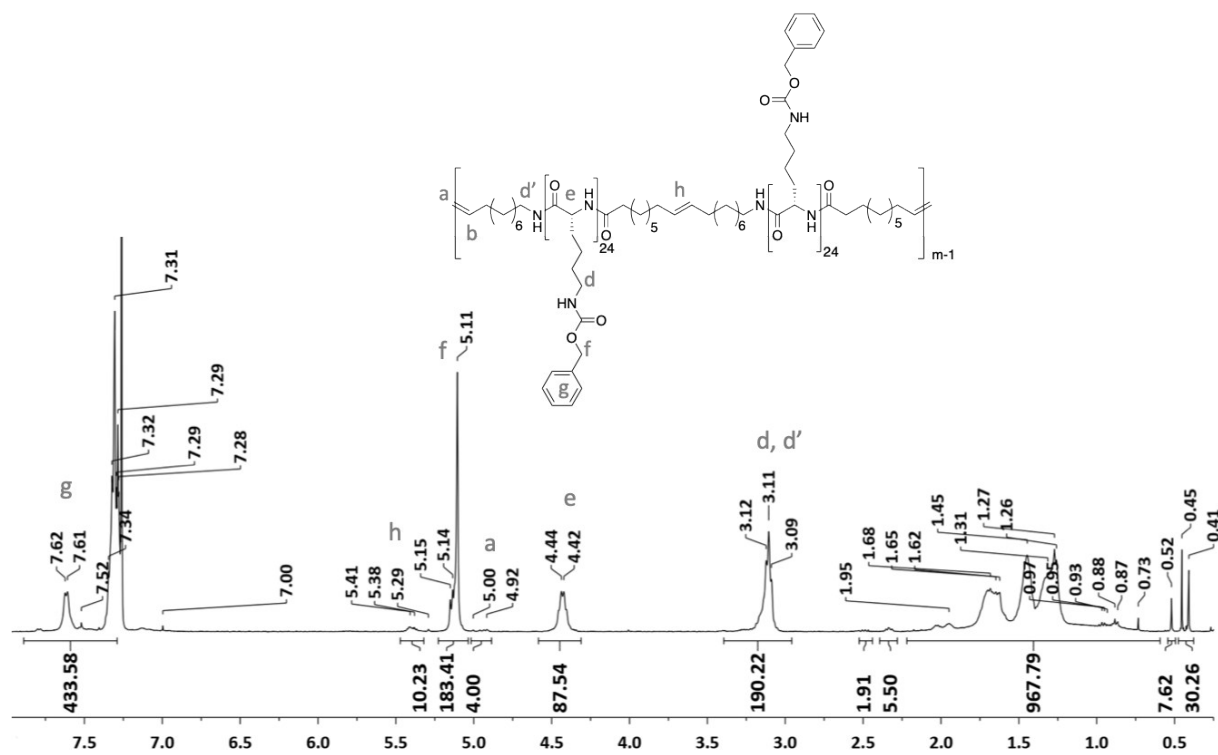


Figure 10S. ¹H-NMR of A-[Lys_{n=24}]_{m=4} (in CDCl₃ and 15 vol.% TFA).

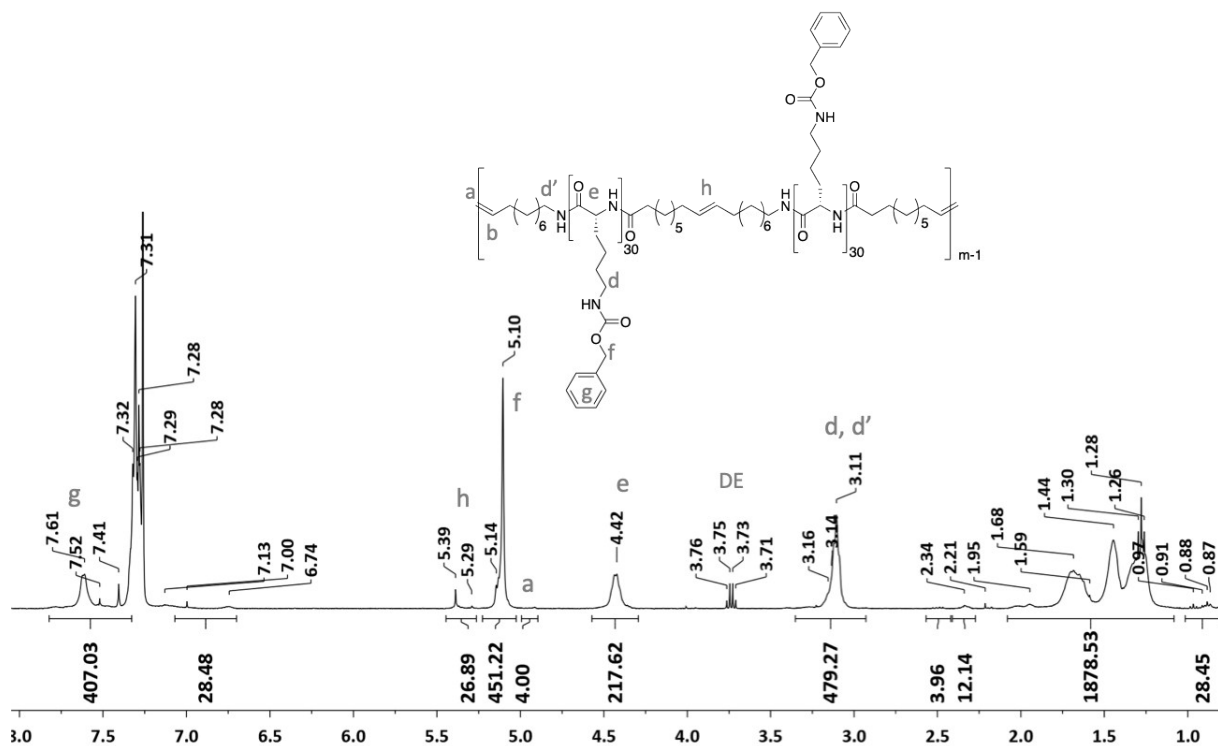


Figure 11S. ¹H-NMR of A-[Lys_{n=30}]_{m=7} (in CDCl₃ and 15 vol.% TFA).

II. MALDI-ToF MS analyses of oligo-L-Lysine(Z)s and ADMET polymers

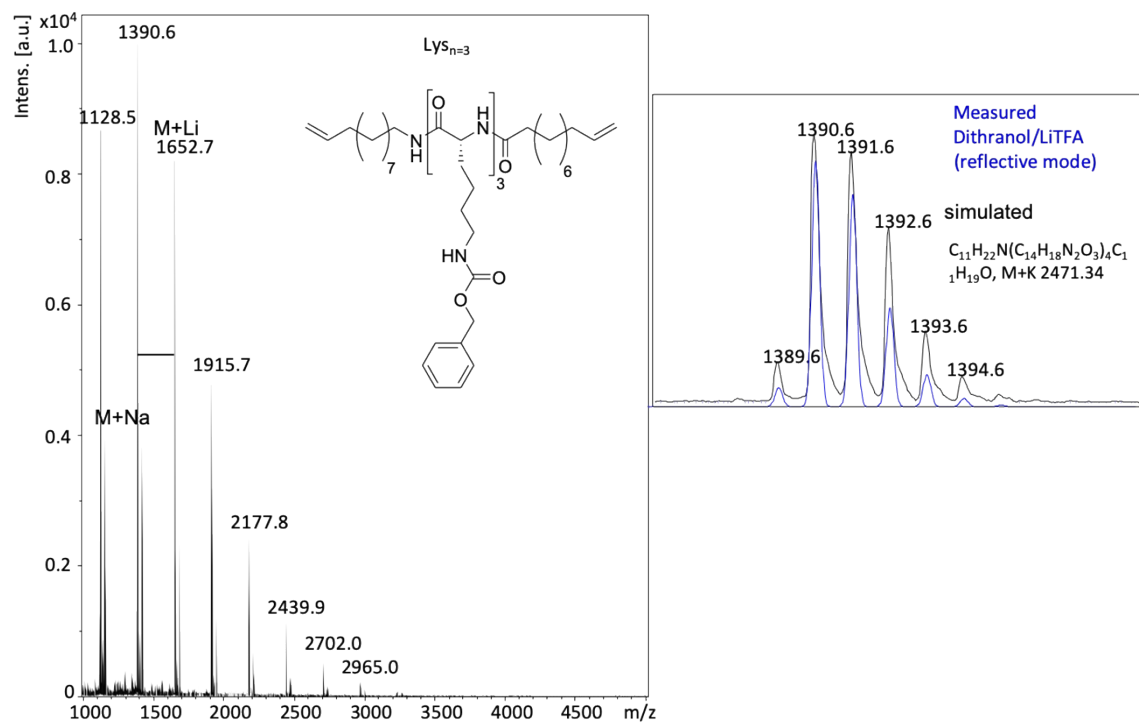


Figure 12S. MALDI-ToF MS spectra of $\text{Lys}_{n=3}$ along with simulated isotopic pattern.

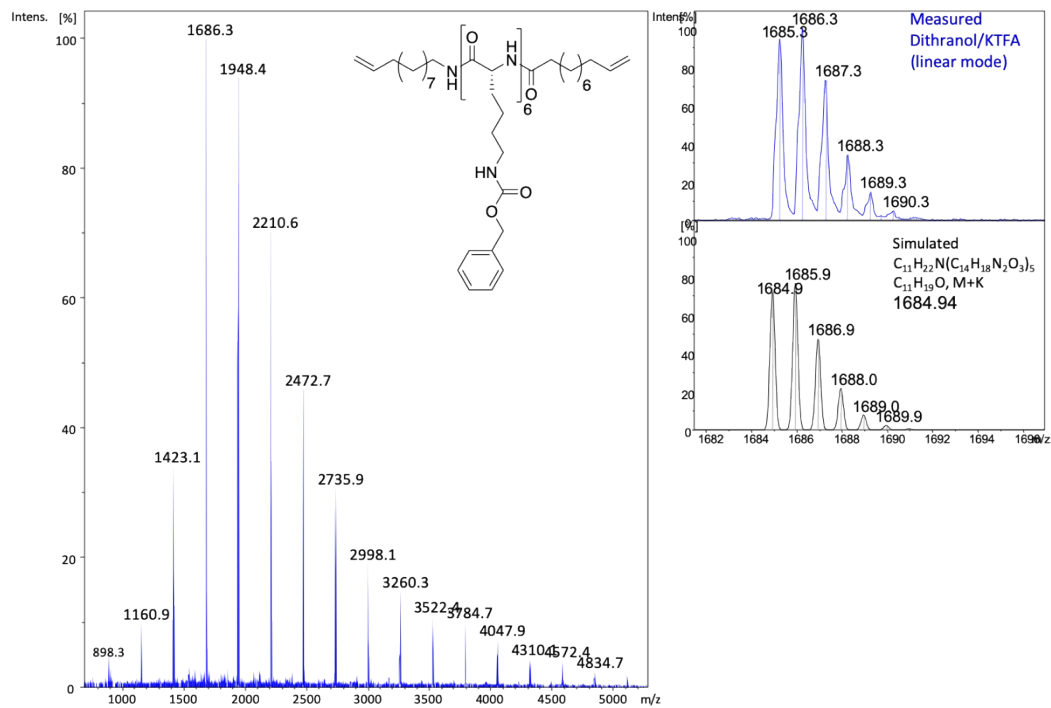


Figure 13S. MALDI-ToF MS spectra of $\text{Lys}_{n=6}$ along with simulated isotopic pattern.

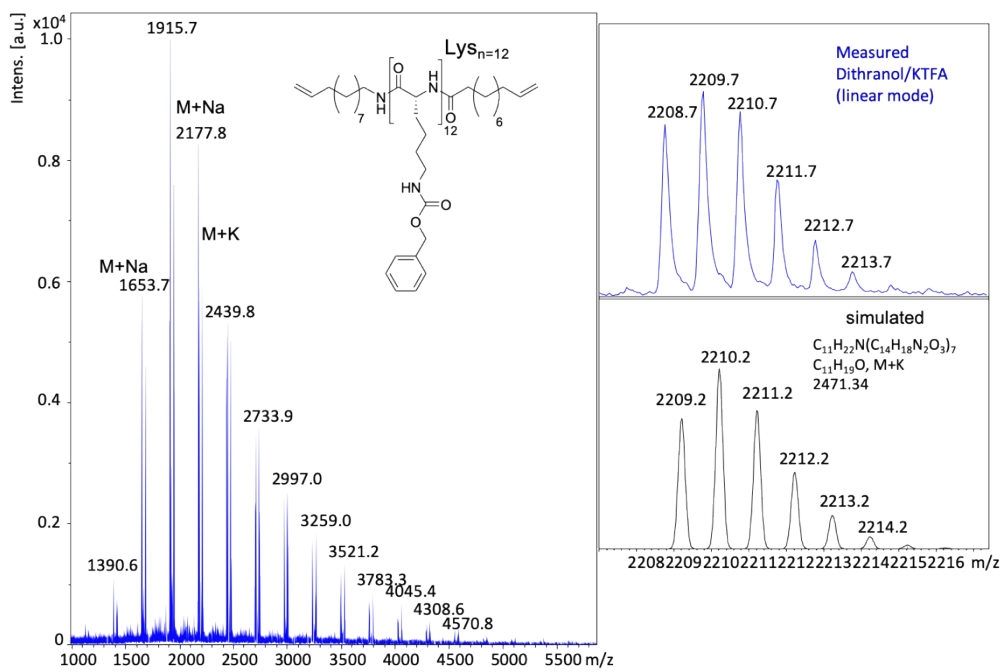


Figure 14S. MALDI-ToF MS spectra of $\text{Lys}_{n=12}$ along with simulated isotopic pattern.

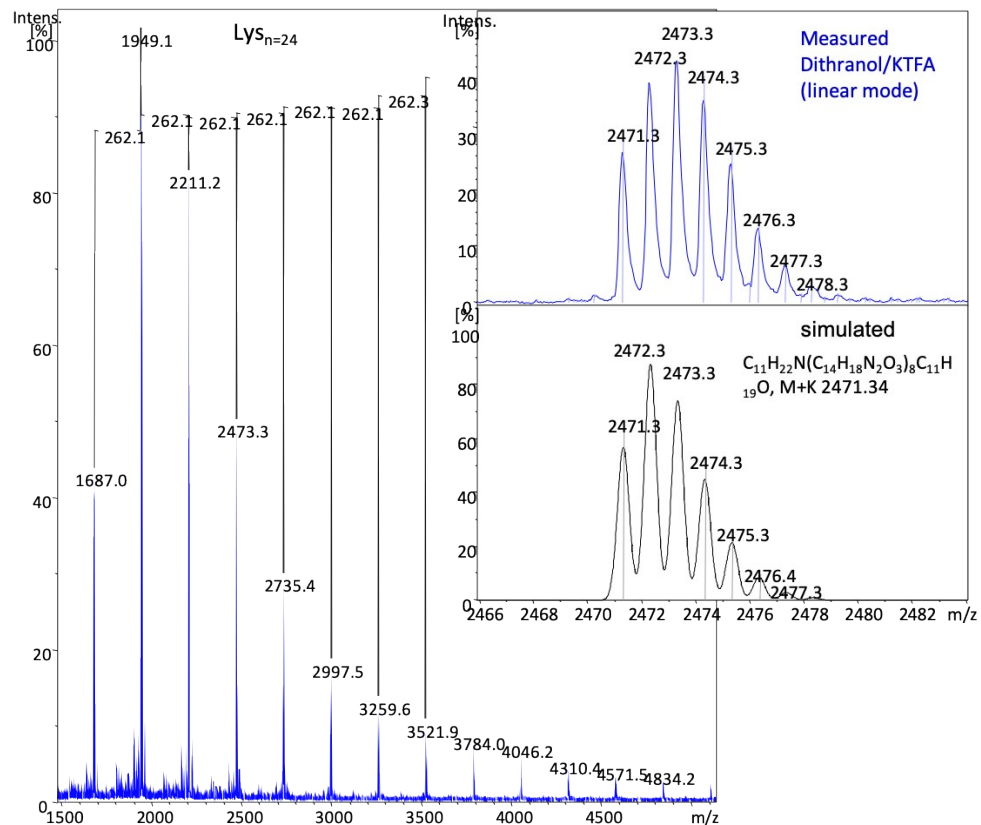


Figure 15S. MALDI-ToF MS spectra of $\text{Lys}_{n=24}$ along with simulated isotopic pattern.

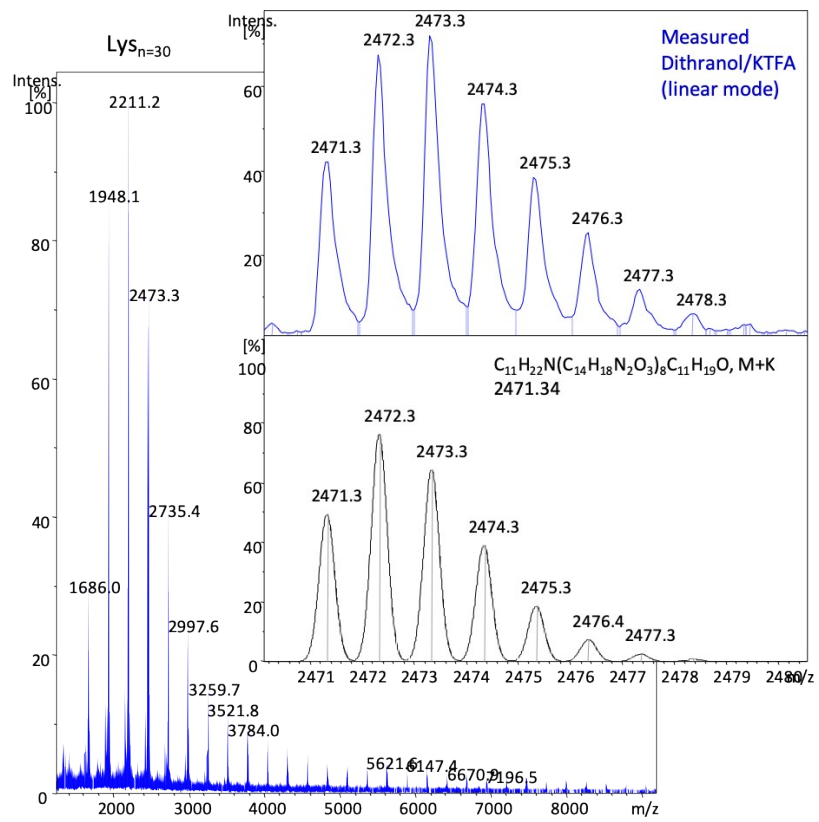


Figure 16S. MALDI-ToF MS spectra of Lys_{n=30} along with simulated isotopic pattern.

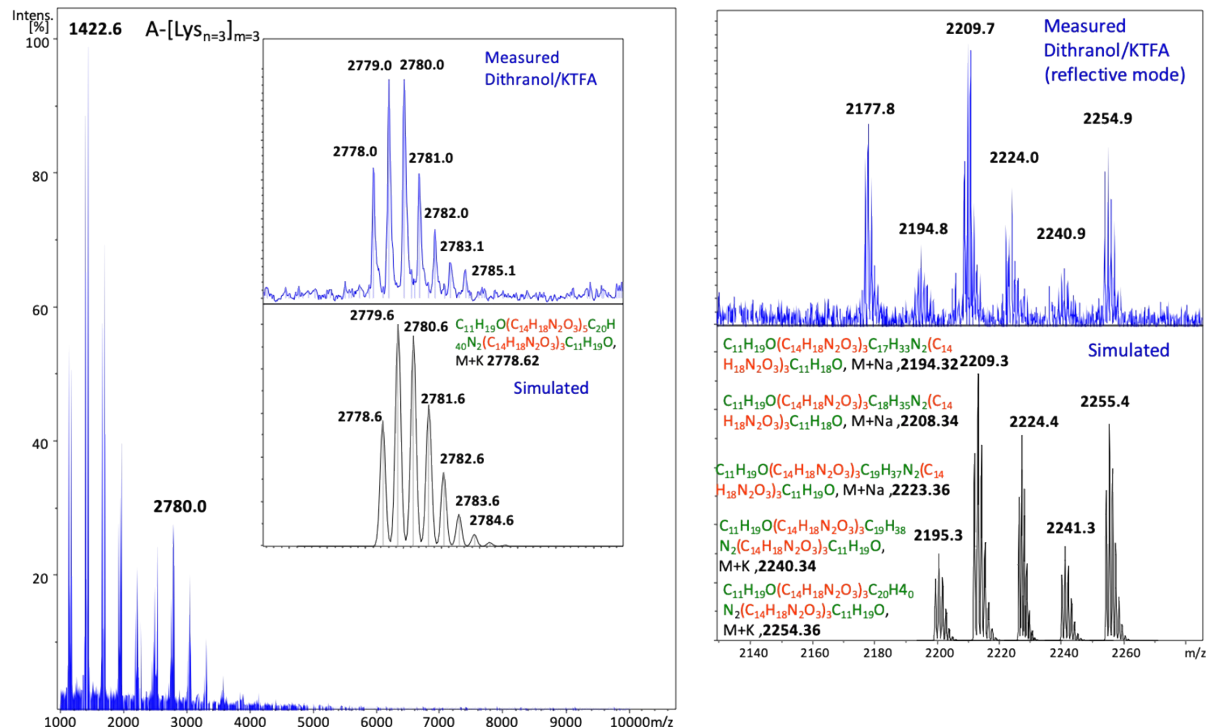


Figure 17S. MALDI-ToF MS spectra of A-[Lys_{n=3}]_{m=3} along with simulated isotopic pattern.

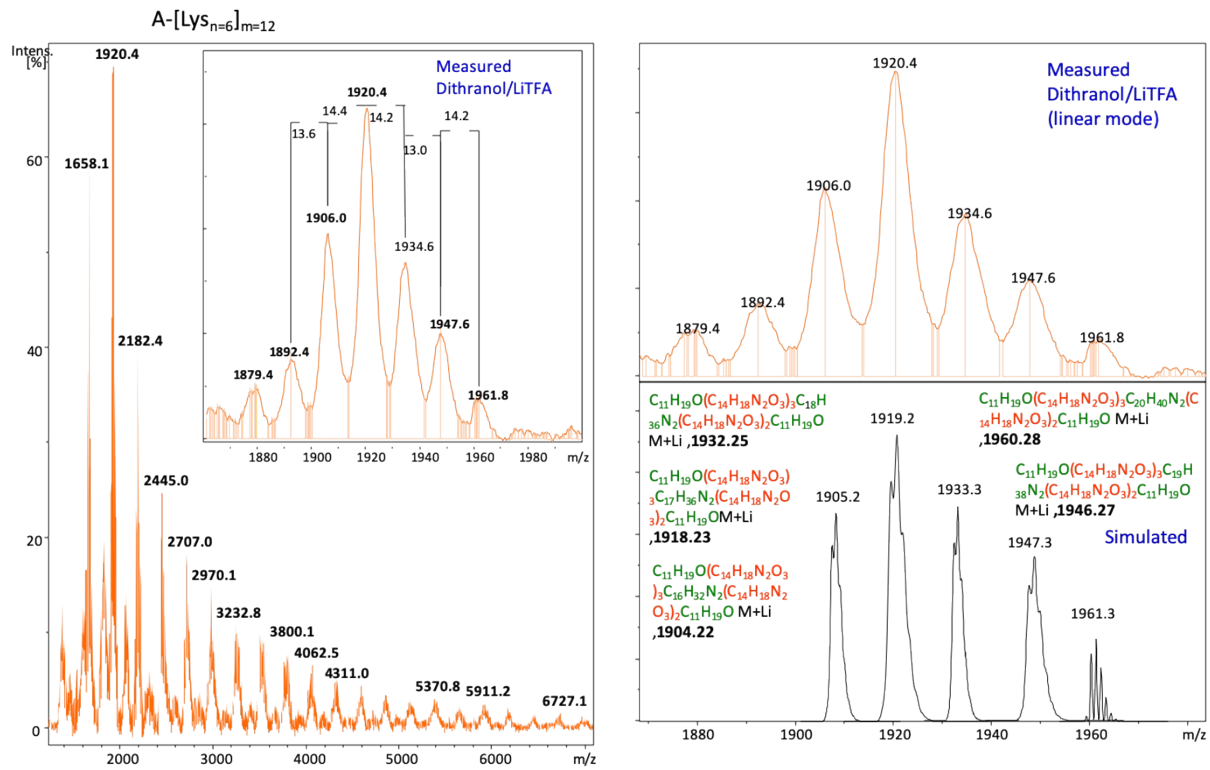


Figure 18S. MALDI-ToF MS spectra of A-[Lys_{n=6}]_{m=12} along with simulated isotopic pattern.

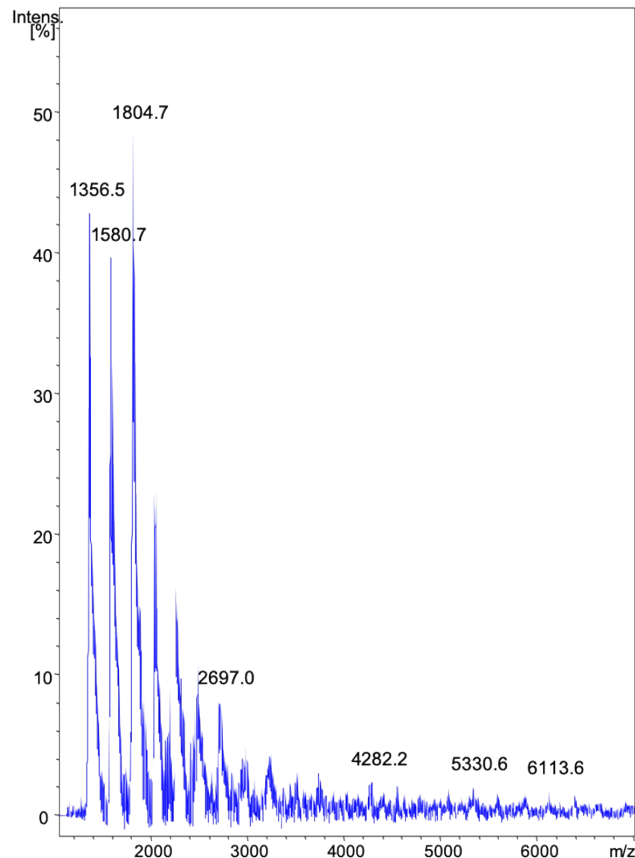


Figure 19S. MALDI-ToF MS spectra of A-[Lys_{n=30}]_{m=7}.

III. CD spectroscopy investigations in TFE

The measured CD spectroscopy data were reported as ellipticity (θ) [mdeg]. The percentage values of α -helicity of the samples were calculated according to the Equation (1S), used for the estimation of the helicity of the peptide chains by Krannig and Sun et al.¹:

Equation (1S) $\alpha\text{-helix}(\%) = (-[\theta]_{222} + 3000)/39\,000 \times 100\%$

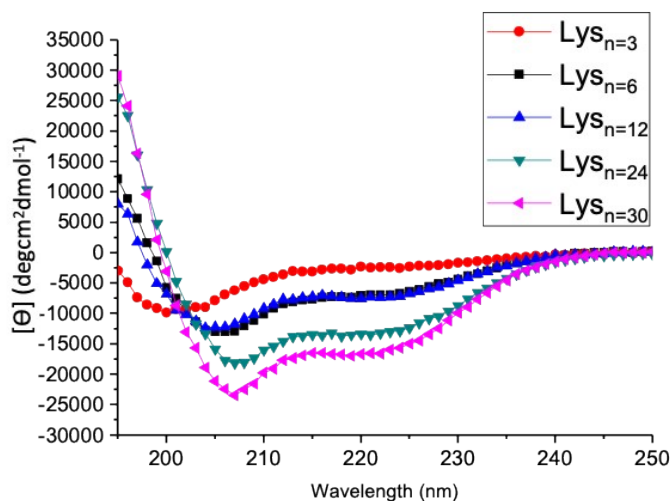


Figure 20S. CD spectra of Lys_ns in TFE (c= 0.2 mg/mL at 20 °C).

IV. IR spectroscopy investigations in TFE

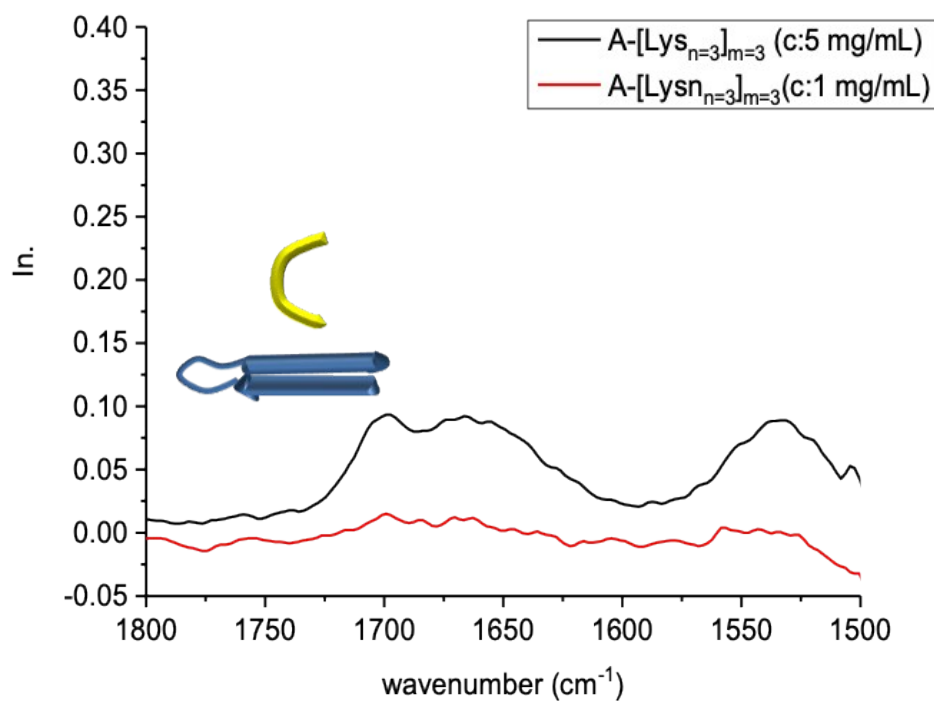


Figure 21S. IR spectra of A-[Lys_{n=3}]_{m=3} (c= 1 mg/mL and c= 5 mg/mL in TFE).

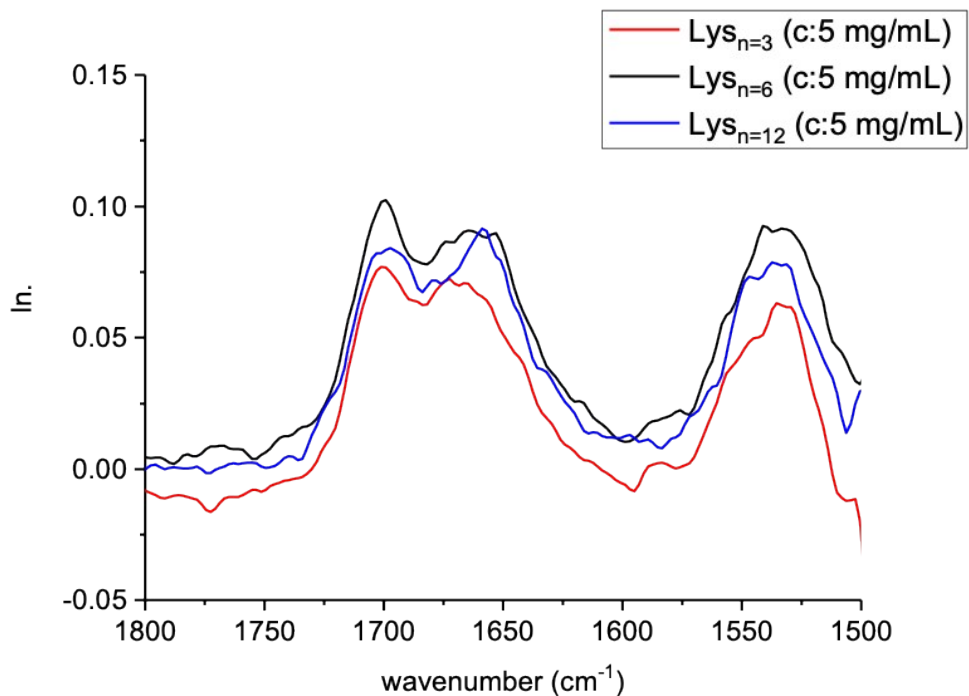


Figure 22S. IR spectra of Lys_{n=3}, Lys_{n=6} and Lys_{n=12} (c: 5 mg/mL in TFE).

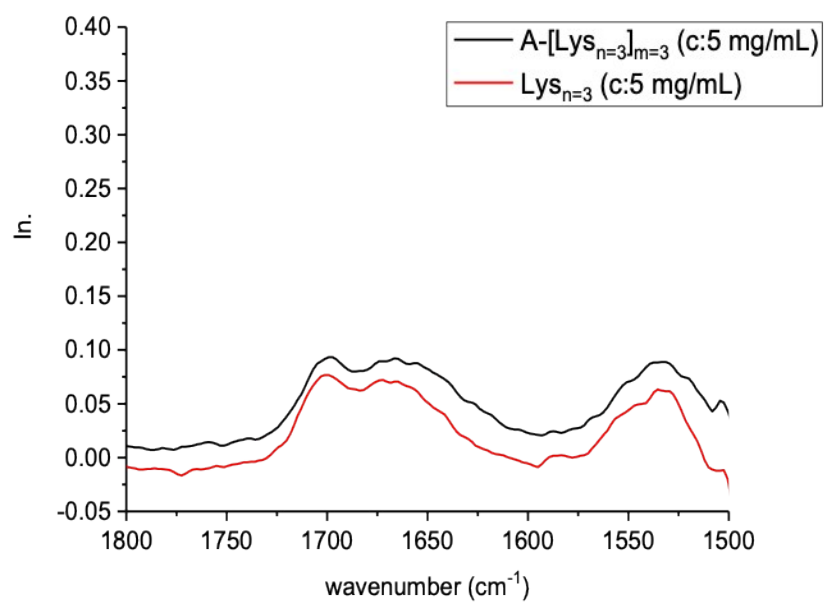


Figure 23S. IR spectra of **Lys_{n=3}** and **A-Lys_{n=3}** (c: 5 mg/mL in TFE).

V. Preparative GPC analyses of ADMET polymer A-[Lys_{n=3}]_{m=3}

Table 1S.

Fractions (F)	A-[Lys _{n=3}] _{m=3}	M _n (g/mol)	M _w (g/mol)	PDI	Fractions of along with and PDI
	F1+F2	NA	NA	NA	
	F3+F4+F5	NA	NA	NA	
	F6-9	NA	NA	NA	
	F10+F12	23 253	28 052	1.206	
	F13+F14	12 773	14 310	1.12	
	F15	9 192	9 892	1.076	
	F16	7 230	7 689	1.063	
	F17	5 780	6 087	1.053	
	F18	4 692	4 933	1.051	
	F19	3 950	4 118	1.043	
	F20	3 418	3 571	1.045	
	F21	2 841	2 969	1.045	
	F22	2 680	2 829	1.056	
	F23	2 383	2 487	1.043	
	F24	2 157	2 228	1.033	
	F25	1 933	1 985	1.027	

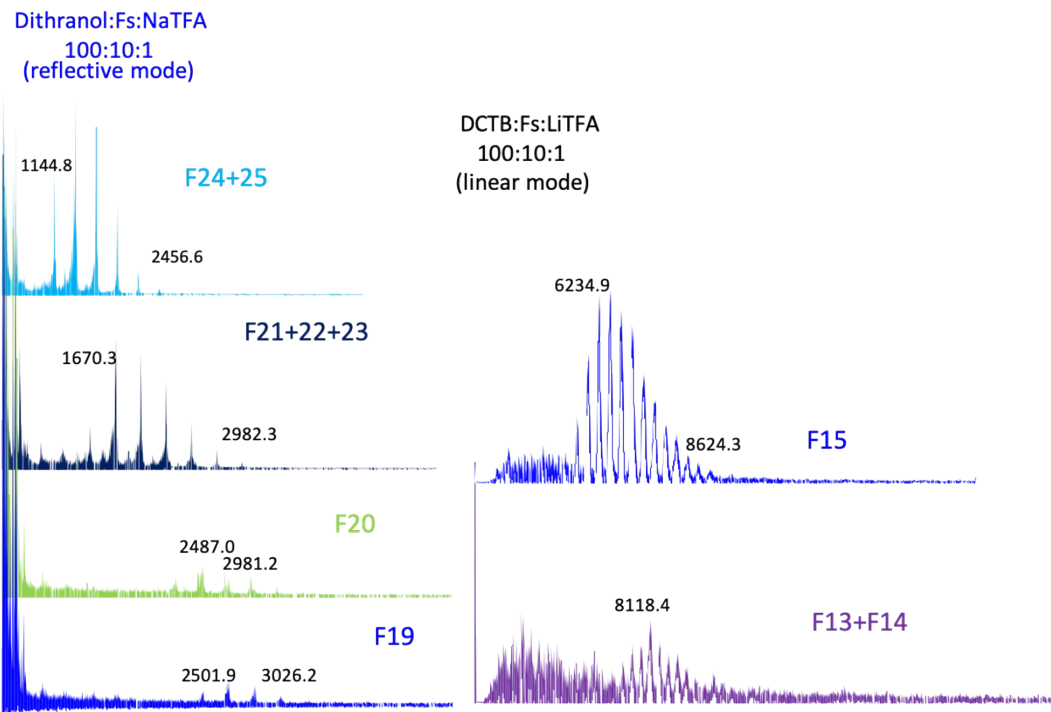


Figure 24S. MALDI spectra of A-[Lys_{n=3}]_{m=3}: F24+F25, F21+F22+F23, F20, F19, F15, F13+F14.

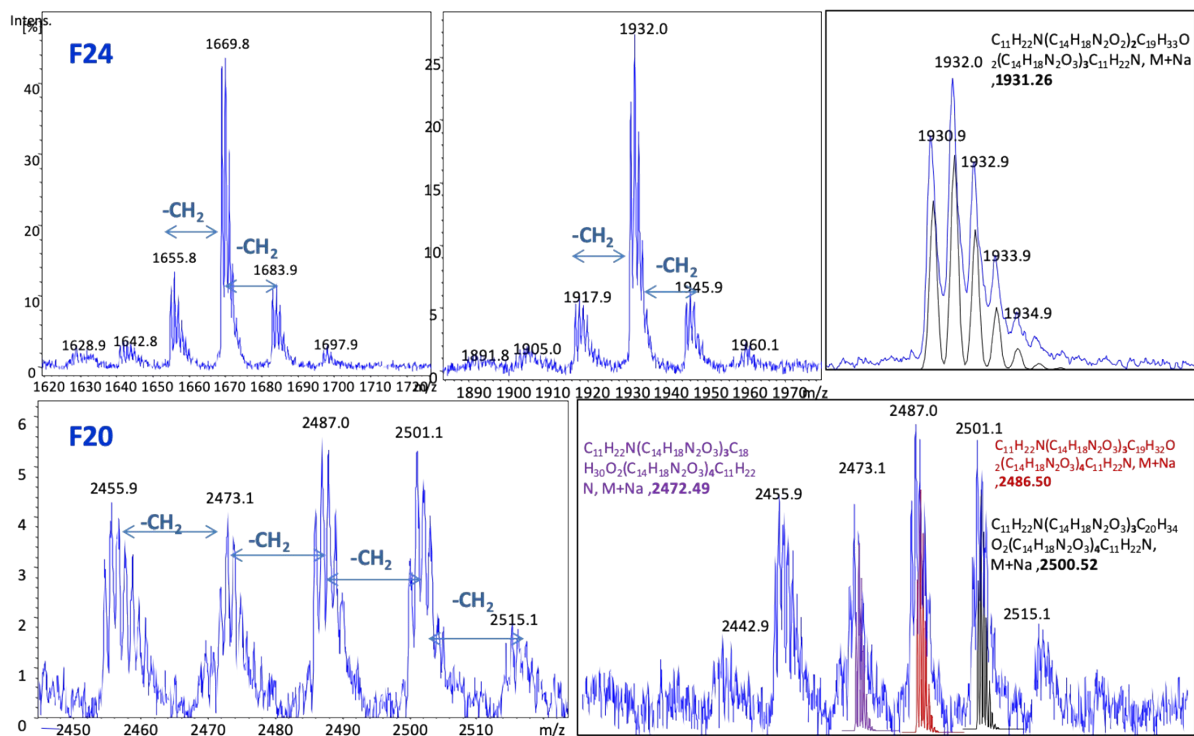


Figure 25S. MALDI-ToF MS spectra of F24 and F20 along with their simulated isotopic patterns.

VI. Preparative GPC analyses of ADMET polymer A-[Lys_{n=24}]_{m=4}

Table 2S. Fractions of A-[Lys_{n=24}]_{m=4} along with their M_w, M_n and PDI values.

A-[Lys _{n=24}] _{m=4}	M _n (g/mol)	M _w (g/mol)	PDI
Fractions (F)	F1-7	15 897	22 654
	F8	13 444	31 193
	F9	23 863	48 096
	F10	22 595	33 355
	F11	22 970	28 973
	F12	23 259	26 916
	F13	19 078	21 952
	F14	15 094	16 855
	F15	12 136	13 022
	F16	10 873	11 640
	F17	8 711	9 528
	F18	7 156	7 711

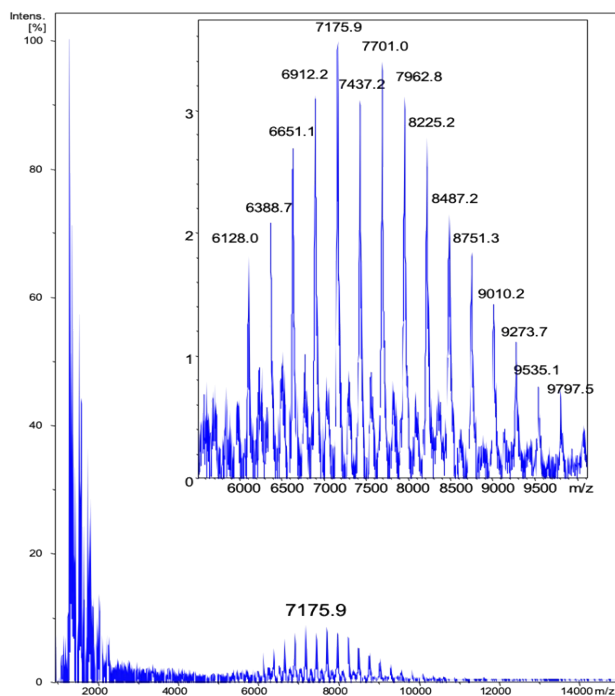


Figure 26S. MALDI-ToF MS spectra of F18.

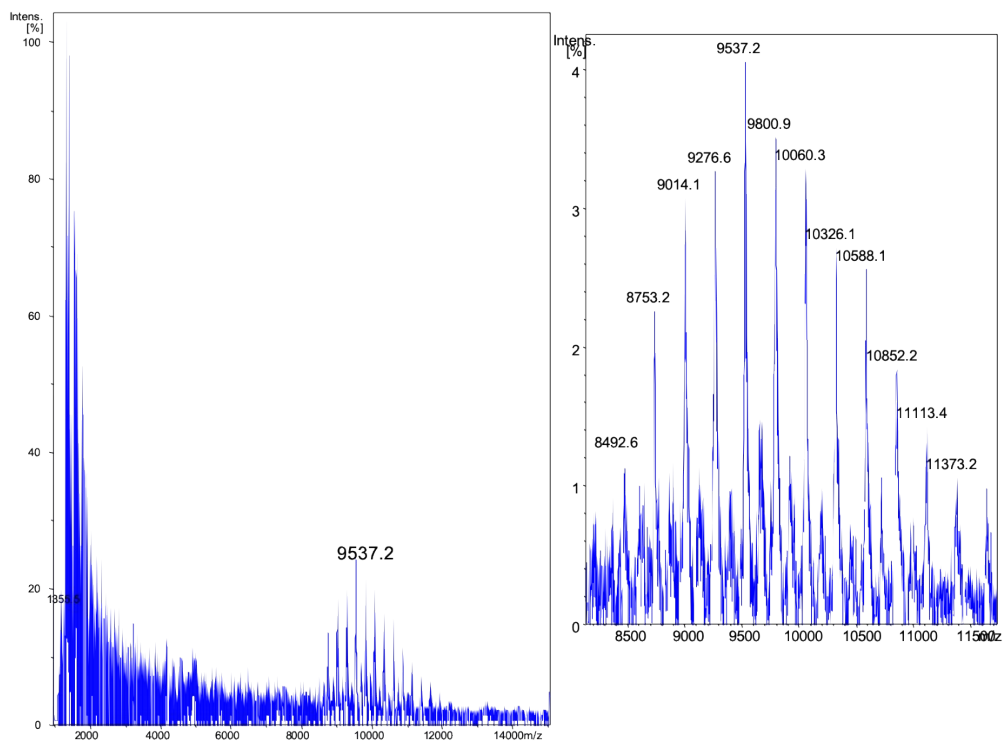


Figure 27S. MALDI-ToF MS spectra of F17.

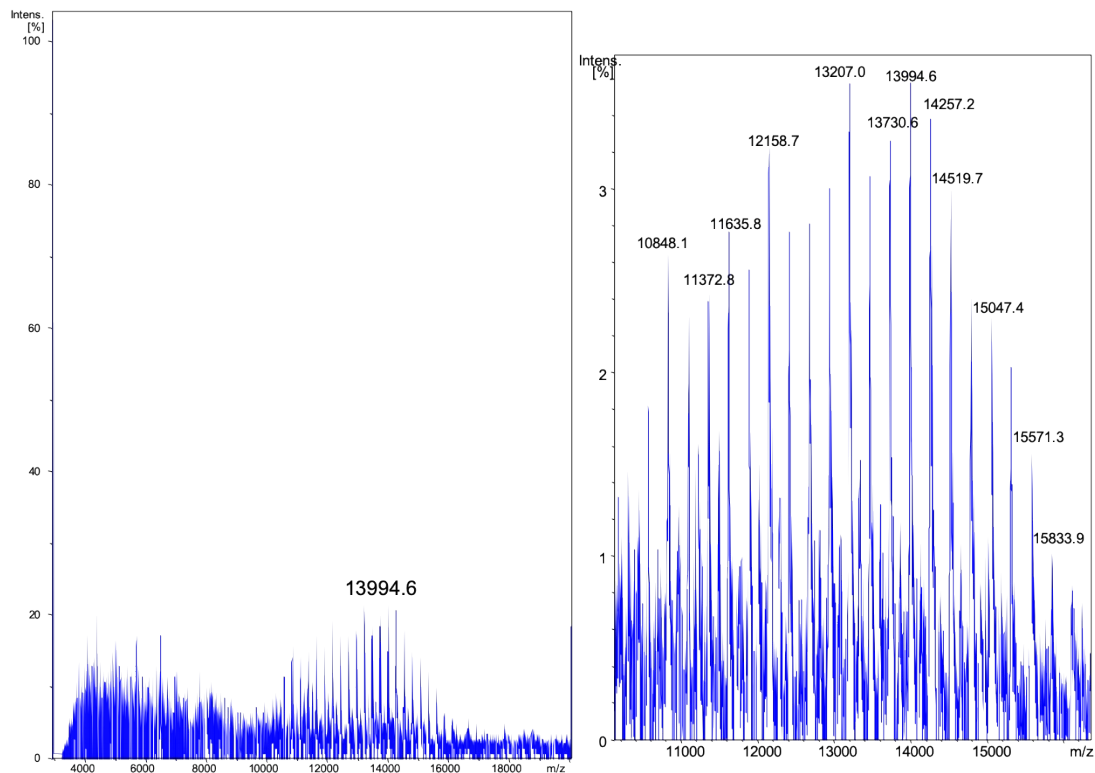


Figure 28S. MALDI-ToF MS spectra of F16.

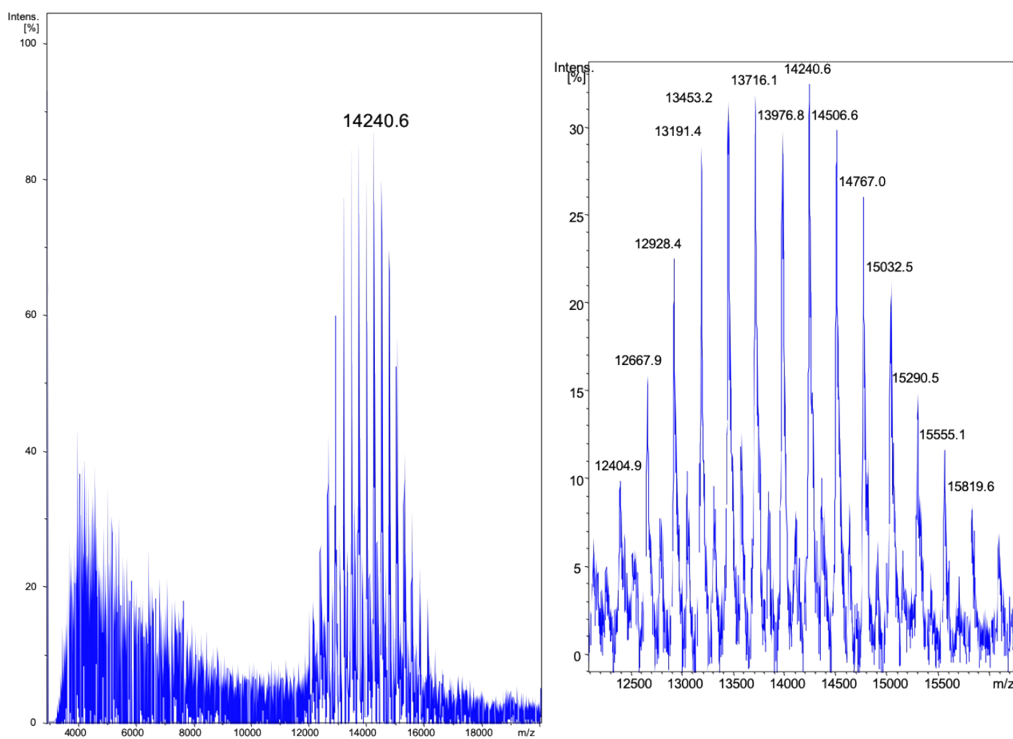


Figure 29S. MALDI-ToF MS spectra of F15.

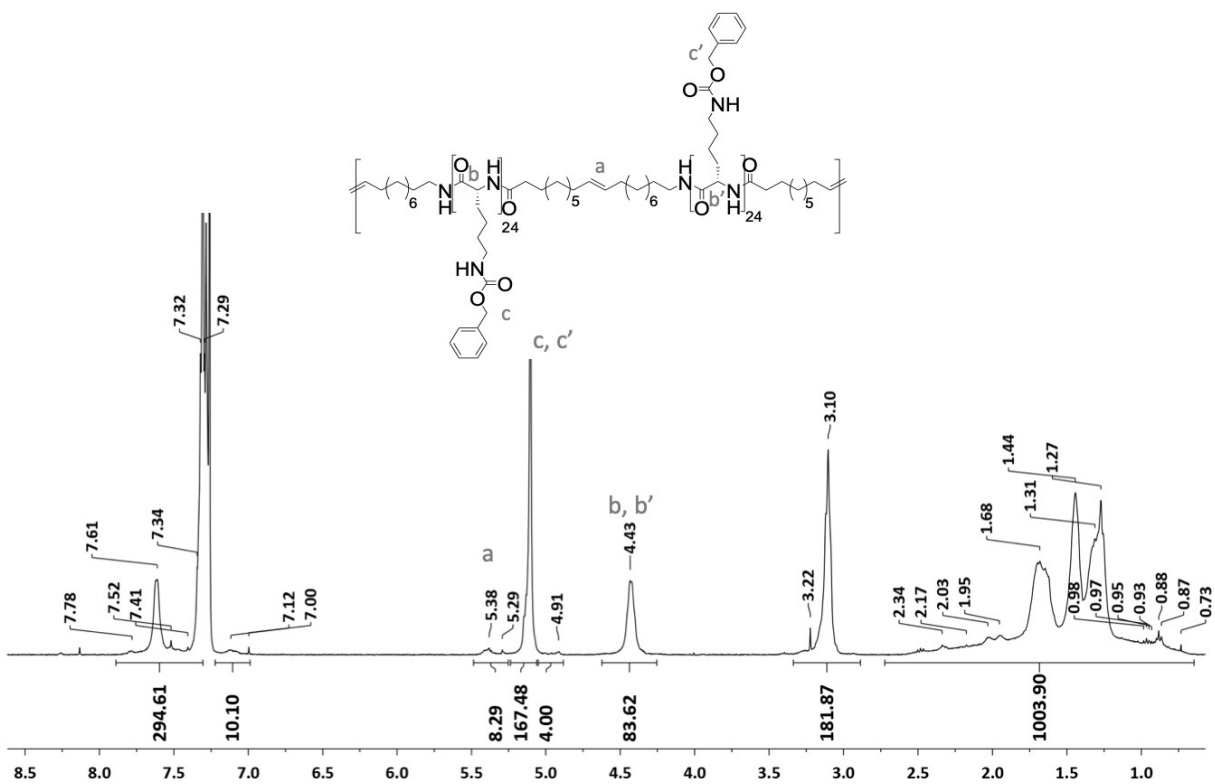


Figure 30S. ^1H -NMR of A-[Lys_{n=24}]_{m=4} fraction, F13.

References

1. K.-S. Krannig, J. Sun and H. Schlaad, *Biomacromolecules*, 2014, **15**, 978-984.